

A q -deformed nonlinear map

Ramaswamy Jaganathan¹ and Sudeshna Sinha²

*The Institute of Mathematical Sciences,
Tharamani, Chennai 600 113, India*

Abstract

A scheme of q -deformation of nonlinear maps is introduced. As a specific example, a q -deformation procedure related to the Tsallis q -exponential function is applied to the logistic map. Compared to the canonical logistic map, the resulting family of q -logistic maps is shown to have a wider spectrum of interesting behaviours, including the co-existence of attractors – a phenomenon rare in one dimensional maps.

Keywords: Nonlinear dynamics, Logistic map, q -Deformation, Tsallis statistics
PACS: 05.45.-a , 05.20.-y , 02.20.Uw

1 Introduction

Emergence of the so-called quantum group structures in certain physical problems has led to studies on several q -deformed physical systems [1]. Enthused over this, and inspired by the elements of Tsallis statistical mechanics [2], we suggest a scheme of q -deformation of nonlinear maps. We then elucidate the general features of a q -deformed logistic map related to the Tsallis q -exponential function, as a concrete illustration of the scheme of q -deformation of nonlinear maps.

Theory of quantum groups turned the attention of physicists to the rich mathematics of q -series, q -special functions, etc., with a history going back to the nineteenth century [3]. The q -deformation of any function involves essentially a modification of it such that in the limit $q \rightarrow 1$ the original function is recovered. Thus there exist several q -deformations of the same function introduced in different mathematical and physical contexts. Here, we are concerned mainly with the q -deformation of real numbers and the exponential function.

Originally, in 1846 Heine deformed a number to a basic number as

$$[n]_q = \frac{1 - q^n}{1 - q}, \quad (1)$$

¹jagan@imsc.res.in

²sudeshna@imsc.res.in

such that $[n]_q \rightarrow n$ when $q \rightarrow 1$. In 1904 Jackson defined a q -exponential function given by

$$E_q(x) = \sum_{n=0}^{\infty} \frac{x^n}{[n]_q!}, \quad (2)$$

with

$$[n]_q! = [n]_q [n-1]_q \cdots [2]_q [1]_q, \quad [0]_q! = 1, \quad (3)$$

as the the solution of the q -differential equation

$$\frac{df(x)}{d_q x} = \frac{f(x) - f(qx)}{(1-q)x} = f(x). \quad (4)$$

It is seen that $E_q(x) \rightarrow \exp(x)$ in the limit $q \rightarrow 1$ when the Jackson q -differential operator $d/d_q x$ also becomes the usual differential operator d/dx .

The mathematics of quantum groups necessitated a new deformation of number as

$$[n]_q = \frac{q^n - q^{-n}}{q - q^{-1}}, \quad (5)$$

which also has the required property that in the limit $q \rightarrow 1$, $[n]_q \rightarrow n$. The associated q -exponential function is given by the same equation (2) but with $[n]_q$ defined according to (5).

In the nonextensive statistical mechanics of Tsallis [2], a new q -exponential function has been introduced as given by

$$e_q^x = (1 + (1-q)x)^{1/(1-q)}, \quad (6)$$

which satisfies the nonlinear equation

$$\frac{df(x)}{dx} = (f(x))^q, \quad (7)$$

and has the required limiting behaviour: $e_q^x \rightarrow \exp(x)$ when $q \rightarrow 1$. This e_q^x plays a central role in the nonextensive statistical mechanics by replacing $\exp(x)$ in certain domains of application; it should be noted that it is natural to define a generalized exponential function as in (6) if we consider the relation

$$e^x = \lim_{N \rightarrow \infty} \left(1 + \frac{x}{N}\right)^N, \quad (8)$$

and regard $1/N$ as a continuous parameter. The formalism of nonextensive statistical mechanics has found applications in a wide range of physical problems [2], including the study of nonlinear maps at the edge of chaos. Here we derive another deformation of numbers based on the Tsallis q -exponential function defined by (6), and use it to study a q -deformed logistic map as an example of the general scheme of q -deformation of nonlinear maps.

2 A q -deformation scheme for nonlinear maps

The series expansion of e_q^x has been presented in [4] as

$$e_q^x = 1 + \sum_{n=1}^{\infty} \frac{Q_{n-1}x^n}{n!}, \quad (9)$$

with

$$Q_n = 1(q)(2q-1)(3q-2)\cdots(nq-(n-1)), \quad n = 0, 1, 2, \dots. \quad (10)$$

Let us take

$$1 - q = \epsilon, \quad (11)$$

and write

$$e_q^x = \tau_\epsilon(x) = (1 + \epsilon x)^{1/\epsilon}. \quad (12)$$

From (9) the series expansion of $\tau_\epsilon(x)$ follows as

$$\tau_\epsilon(x) = \sum_{n=0}^{\infty} \frac{T_n x^n}{n!}, \quad (13)$$

with

$$T_n = \begin{cases} 1, & \text{for } n = 0, \\ 1(1-\epsilon)(1-2\epsilon)\cdots(1+(1-n)\epsilon), & \text{for } n \geq 1. \end{cases} \quad (14)$$

Comparison of (2) and (13) suggests that we have here another deformation of numbers:

$$[n]_\epsilon = \frac{n}{1 + (1-n)\epsilon}, \quad (15)$$

such that

$$\lim_{\epsilon \rightarrow 0} [n]_\epsilon = n. \quad (16)$$

Then, we have

$$\tau_\epsilon(x) = \sum_{n=0}^{\infty} \frac{x^n}{[n]_\epsilon!}, \quad (17)$$

exactly analogous to the expression for $E_q(x)$ in (2).

It is usual to extend the deformation rule for integers, such as in (1) or (5), to any X by substituting X for n . For example, the commutation relations of the q -deformed $su(2)$ algebra are given by

$$J_0 J_\pm - J_\pm J_0 = \pm J_0, \quad J_+ J_- - J_- J_+ = [2J_0]_q, \quad (18)$$

where $[2J_0]_q$ is obtained from the definition of $[n]_q$ in (5) by replacing n by $2J_0$, i.e., $[2J_0]_q = (q^{2J_0} - q^{-2J_0})/(q - q^{-1})$. Thus, we take that for any real number x

$$[x]_\epsilon = \frac{x}{1 + \epsilon(1 - x)}. \quad (19)$$

Note that $[x]_\epsilon \rightarrow x$ when $\epsilon \rightarrow 0$. Further, $[0]_\epsilon = 0$ and $[1]_\epsilon = 1$, as in the case of other deformations in (1) and (5). Here after, we shall denote $[x]_\epsilon$ simply as $[x]$ and take it to be defined by (19) unless stated otherwise.

The q -deformation scheme for discrete dynamical maps we suggest is the following. For the one-dimensional map

$$x_{n+1} = f(x_n) \quad (20)$$

the q -deformed version is

$$x_{n+1} = f([x_n]_q), \quad (21)$$

where $[x_n]_q$ is, in general, any q -deformed value of x_n ; essentially a q -deformed map is obtained by composing the given map with a basic number deforming map. For example, the q -deformed logistic map, corresponding to the definition of deformed x as in (19), is:

$$x_{n+1} = a[x_n](1 - [x_n]) = F(x_n) = \frac{a(1 + \epsilon)x_n(1 - x_n)}{(1 + \epsilon(1 - x_n))^2}. \quad (22)$$

We shall refer to the map in (22) simply as the q -logistic map. When $\epsilon \rightarrow 0$ the q -logistic map becomes the usual logistic map. In the following we present the interesting properties of the q -logistic map in detail.

3 The q -logistic map

Figure 1 displays the q -logistic map function in (22),

$$F(x) = \frac{a(1 + \epsilon)x(1 - x)}{(1 + \epsilon(1 - x))^2}, \quad (23)$$

for $a = 4$. The usual logistic map corresponds to $\epsilon = 0$. It is clear that as ϵ moves away from 0 the map gets more skewed. The map is skewed to the right for positive ϵ and to the left for negative ϵ . The lower and upper bounds for ϵ are, respectively, -1 and ∞ where $F(x)$ vanishes. Taking the domain of the q -logistic map the same as for the logistic map, namely the interval $[0, 1]$, it is found that the range of the q -logistic map is the same as for the logistic map. This is so because over the interval $[0, 1]$ the map function $F(x)$ has no singularity for $-1 < \epsilon < \infty$, and $x \leq [x] \leq 1$ for $-1 \leq \epsilon < 0$ and $[x] \leq x$ for $\epsilon \geq 0$. There is one important qualitative difference between the usual logistic map and its deformed version. *The deformed map is concave in parts of x -space, whereas the usual logistic map is always convex.* Note that the form of

the q -logistic map is similar to certain maps used to model population dynamics, such as the Bellows map: $f(x) = rx/(1+x^b)$, and the Moran-Ricker exponential map: $f(x) = x \exp\{r(1-x)\}$, where r is the nonlinearity parameter leading from periodic behavior to chaos [5].

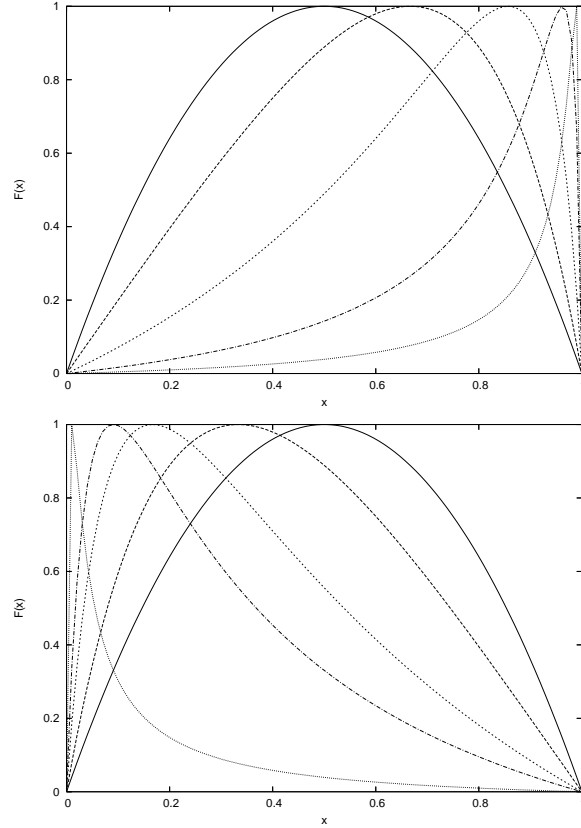


Figure 1: Graph of the q -logistic map function $F(x)$ for $a = 4$. The solid curve is for $\epsilon = 0$ (usual logistic map). The dashed curves skewed increasingly to the right in the top panel are for $\epsilon = 1, 5, 25, 100$. The dashed curves skewed increasingly to the left in the bottom panel are for $\epsilon = -0.5, -0.8, -0.9, -0.99$.

The fixed points of the map in (22) are given by

$$x^* = \frac{a(1+\epsilon)x^*(1-x^*)}{(1+\epsilon(1-x^*))^2}. \quad (24)$$

This has one solution at $x^* = 0$. For $x^* \neq 0$ the above equation becomes

$$1 = \frac{a(1 + \epsilon)(1 - x^*)}{(1 + \epsilon(1 - x^*))^2}. \quad (25)$$

Substituting $1 - x^* = y$ in this equation gives

$$(1 + \epsilon y)^2 = a(1 + \epsilon)y, \quad (26)$$

or

$$\epsilon^2 y^2 + (2\epsilon - a(1 + \epsilon))y + 1 = 0. \quad (27)$$

So

$$y = \frac{1}{2\epsilon^2} \left\{ a(1 + \epsilon) - 2\epsilon \pm \sqrt{a^2(1 + \epsilon)^2 - 4a\epsilon(1 + \epsilon)} \right\} \quad (28)$$

Thus, the fixed points $\{x^*\}$ of the q -logistic map are :

$$x^* = 0, \quad (29)$$

$$x^*_+ = \left(1 - \frac{1}{2\epsilon^2} \{a(1 + \epsilon) - 2\epsilon\} \right) + \frac{1}{2\epsilon^2} \sqrt{a^2(1 + \epsilon)^2 - 4a\epsilon(1 + \epsilon)}, \quad (30)$$

$$x^*_- = \left(1 - \frac{1}{2\epsilon^2} \{a(1 + \epsilon) - 2\epsilon\} \right) - \frac{1}{2\epsilon^2} \sqrt{a^2(1 + \epsilon)^2 - 4a\epsilon(1 + \epsilon)}. \quad (31)$$

Figure 2 displays the numerically obtained fixed points of the map for $a = 1.5$ for different values of ϵ . These coincide exactly with the analytical expression for x^*_+ above. It should be noted that for a given value of a only for some range of values of ϵ both x^*_+ and x^*_- lie within the range of $F(x)$.

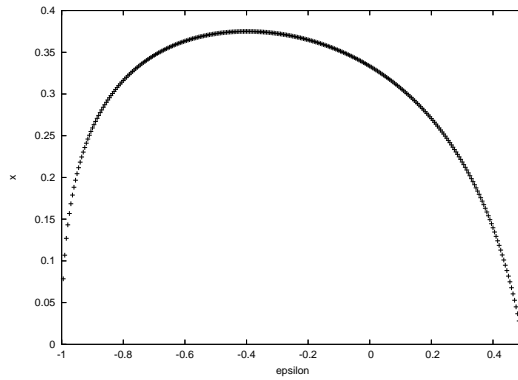


Figure 2: Bifurcation diagram of the map with respect to ϵ for $a = 1.5$

Figure 3 gives the bifurcation diagram of the map for $a = 3$ with respect to different values of ϵ . It is clear that the fixed point x^*_+ loses stability for negative

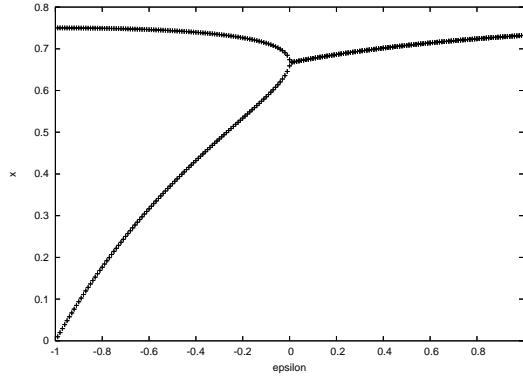


Figure 3: Bifurcation diagram of the map with respect to ϵ for $a = 3$

ϵ . This can be straight-forwardly understood from the absolute magnitude of $F'(x^*)$, which crosses the value 1 at $\epsilon = 0$ when $a = 3$.

Figure 4 gives the bifurcation diagram of the map for $a = 3.5$ with respect to different values of ϵ . In this case the usual logistic map ($\epsilon = 0$) yields a 4-cycle. As ϵ increases there is a reverse bifurcation and the 2-cycle gains stability, followed by the fixed point. However, note that the fixed point at $x^* = 0$ also gains stability when ϵ is sufficiently high, and we have a *co-existence* of attractors, namely, the fixed point at 0 co-exists, first with the 2-cycle and then with the fixed point x_+^* .

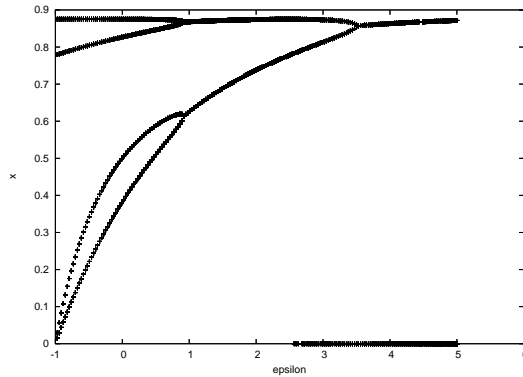


Figure 4: Bifurcation diagram of the map with respect to ϵ for $a = 3.5$

Similar features, namely reverse bifurcations in ϵ -space, and the co-existence

of the fixed point $x^* = 0$ with other dynamical behaviour at high ϵ , are observed for larger values of a as well (see Figs. 5-9).

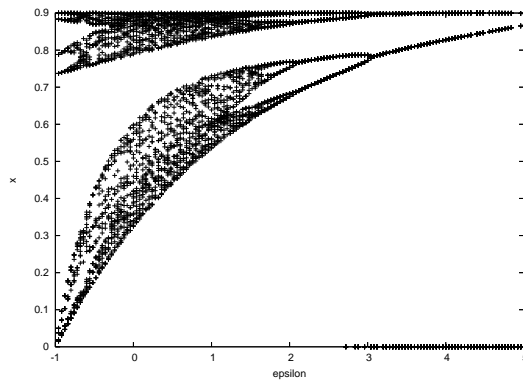


Figure 5: Bifurcation diagram of the map with respect to ϵ for $a = 3.6$

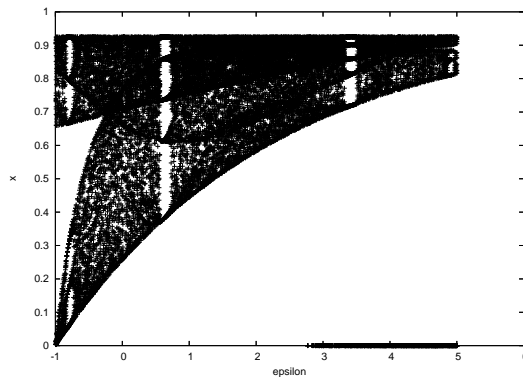


Figure 6: Bifurcation diagram of the map with respect to ϵ for $a = 3.7$

4 Co-existence of attractors

It is clearly evident from the above that the q -logistic map offers a rare example of multiple attractors in a one-dimensional smooth unimodal system [6]. The fixed point at $x^* = 0$ co-exists with other kinds of dynamical behaviour when ϵ is sufficiently high. The basin of attraction for $x^* = 0$, as reflected in the

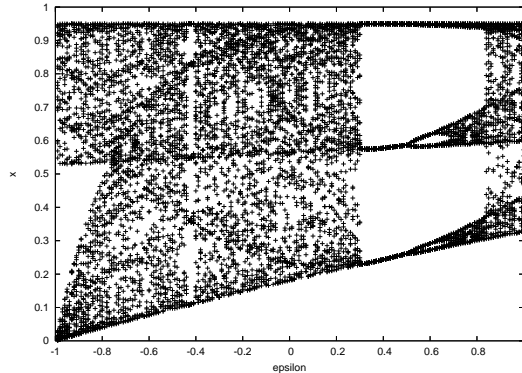


Figure 7: Bifurcation diagram of the map with respect to ϵ for $a = 3.8$

fraction of initial conditions which are attracted to 0, monotonically increases with ϵ . Figures 10-12 show the basins of attraction for the fixed point $x^* = 0$ for three different values of a . It is clear that this fixed point is a global attractor at sufficiently high ϵ . In Figure 12 for $a = 4$ clearly there is a sharp transition to a global attractor (where all initial conditions lead to $x^* = 0$) at around $\epsilon \sim 3$. So, the fully chaotic logistic map under deformation with positive ϵ can yield stable fixed points.

The co-existence of attractors is also evident from the bifurcation diagrams for the map with respect to a for different values of ϵ displayed in Figs. 13-15.

Figures 16-18 display the Lyapunov exponents, obtained from trajectories arising from different initial conditions. Fig. 16 displays the exponents with respect to ϵ for $a = 3.6$, and it shows two branches of Lyapunov exponents arising from different initial conditions, after $\epsilon \sim 2.5$. Both these co-existing exponents are below 0, indicating the co-existence of two regular dynamical behaviours. This is borne out in Fig. 5 – from where it is clearly evident that after $\epsilon \sim 2.5$ the fixed point $x^* = 0$ co-exists with a 2-cycle.

In Fig. 17 one observes, for certain ϵ , both positive and negative Lyapunov exponents are obtained for different initial conditions. This signals a co-existence of chaos and regular dynamics, as is clearly borne out by the bifurcation diagram in Fig. 6.

From the Lyapunov exponents shown in Fig. 18 and the corresponding bifurcation sequence in Fig. 9, it is clear that for $a = 4$, we have a global chaotic attractor extending over the entire interval for the usual logistic map ($\epsilon = 0$), but obtain a global attractor at $x^* = 0$ for $\epsilon > 3$. So q -deformation of a chaotic map can lead to stable fixed points.

The co-existence of attractors for the q -logistic map can be understood as follows. Consider, for example, the case of $a = 3.7$ and $\epsilon = 7$ where a 2-cycle

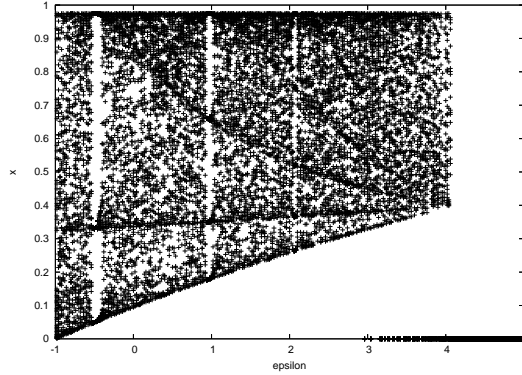


Figure 8: Bifurcation diagram of the map with respect to ϵ for $a = 3.9$

co-exists with the fixed point $x^* = 0$. Figure 19 shows the form of the dynamical evolution function $F(x)$ with respect to x for these values of a and ϵ . The figure also displays the $F(x) = x$ line and the $F(x) = x_-^*$ line. The intersection of the former with the $F(x)$ curve yields the fixed points $x^* = 0$, x_-^* and x_+^* . The intersection of the latter with the $F(x)$ curve yields the two pre-images for the fixed point x_-^* . One pre-image is simply x_-^* (i.e., it is also on the 45° line) as it is a fixed point solution. The other pre-image is given by :

$$F^{-1}(x_-^*) = \frac{(2\epsilon\epsilon'x_-^* + a') + \sqrt{(2\epsilon\epsilon'x_-^* + a')^2 - 4(\epsilon^2x_-^* + a')\epsilon'^2x_-^*}}{2(\epsilon^2x_-^* + a')} \quad (32)$$

where $\epsilon' = 1 + \epsilon$ and $a' = a\epsilon'$. This marks the beginning of the interval $[F^{-1}(x_-^*), 1]$ which maps on to the interval $[0, x_-^*]$ in the consequent iteration. These two intervals are dynamically connected and all points in it are attracted to the fixed point $x^* = 0$. Notice however that the interval $[x_-^*, F^{-1}(x_-^*)]$ is never mapped to the other two. In fact it always maps on to itself. Basically the $F(x)$ in the range $[x_-^*, F^{-1}(x_-^*)]$ will lie in the interval $[x_-^*, F_{max}]$, where F_{max} is the maximum of the map $F(x)$. Whenever $F_{max} < F^{-1}(x_-^*)$, the middle segment will map onto itself. When this happens the dynamics in this segment will be distinct from that in the other two, and we will have a co-existence of dynamical attractors. Figure 19 also shows the numerically obtained basin of attraction for the fixed point $x^* = 0$ as a black bar on the x -axis, and clearly it falls exactly in the intervals outlined above.

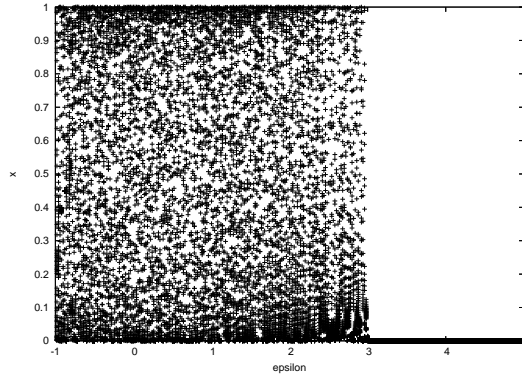


Figure 9: Bifurcation diagram of the map with respect to ϵ for $a = 4$

5 Conclusions

To summarize, we have introduced a scheme of q -deformation of nonlinear maps, enthused over studies on several q -deformed physical systems related to quantum group structures and inspired by the mathematical basis of Tsallis statistical mechanics. We characterized the scheme in detail with reference to the logistic map. The resulting family of q -logistic maps has been found to have an interestingly wide spectrum of behaviours, compared to the usual logistic map. In particular one observed co-existence of attractors – a phenomenon rare in one dimensional maps.

One can also study the q -deformations of maps following other deformation schemes, like based on (1) or (5). We feel that the study of such families of deformed maps should be profitable for analytical modeling of several phenomena, as one parameter, namely the deformation parameter, can be used to fit a large range of functional forms, as evident from Fig. 1. For instance, it is seen that the experimentally constructed one dimensional map for the Belousov-Zhabotinskii reaction in a stirred chemical reactor [7] has a striking similarity to the q -logistic map in Fig. 1 for negative epsilon value. Clearly there are many interesting areas of research for further exploration. One can study the q -deformations of the various other nonlinear maps (one or higher dimensional) and coupled map systems. Further, in higher dimensional cases and coupled map systems one can experiment with different deformation parameters (ϵ) for different variables and for different maps coupled in the system. In conclusion, q -deformation allows us to generate interesting families of maps and has potential utility in constructing iterated functional schemes to model low dimensional dynamical phenomena.

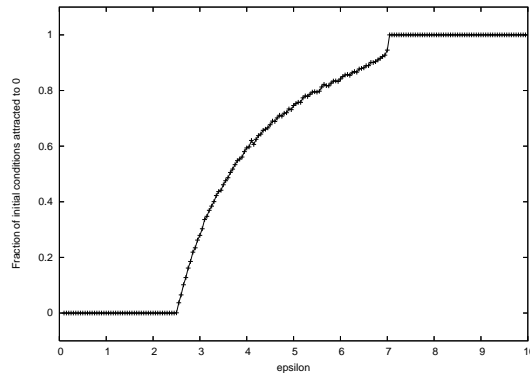


Figure 10: Fraction of initial conditions attracted to the fixed point $x^* = 0$, for varying values of ϵ for $a = 3.5$.

References

- [1] See, e.g., L. Castellani, J. Wess (Eds.), Quantum Groups and their Applications in Physics, Proc. International School of Physics “Enrico Fermi” - Course CXXVII, IOS Press, Amsterdam, 1996; M. Chaichian, A. Demichev, Introduction to Quantum Groups, World Scientific, Singapore, 1996; D. Bonatsos, C. Daskaloyannis, Prog. Part. Nucl. Phys. 43 (1999) 537; D. Bonatsos, N. Karoussos, P.P. Raychev, R.P. Roussev, Cond. Matt. Theor. 15 (2000) 25;
- [2] C. Tsallis, J. Stat. Phys. 52 (1988) 479; and see, e.g., S.R.A. Salinas, C. Tsallis (Eds.), Nonextensive Statistical Mechanics and Thermodynamics, Braz. J. Phys. 29 (1999) No.1; M. Gell-Mann, C. Tsallis (Eds.), Nonextensive Entropy - Interdisciplinary Applications, Oxford University Press, New York, 2004; G.F.J. Ananos, C. Tsallis, cond-mat/0401276.
- [3] See, e.g., G. Gasper and M. Rahman, Basic Hypergeometric Series, Cambridge University Press, Cambridge, 1990.
- [4] E.P. Borges, J. Phys. A 31 (1998) 5281.
- [5] T.S. Bellows, J. Anim. Ecol. 50 (1981) 139; P.A.P. Moran, Biometrics 6 (1950) 250; W.E. Ricker, J. Fish. Res. Board Can. 11 (1954) 559; and see, e.g., S. Sinha, S. Parthasarathy, Proc. Natl. Acad. Sci. USA 93 (1996) 1504.
- [6] One known example of a 1-dimensional system with co-existing attractors is the Gaussian map: $x_{n+1} = a + \exp(-bx_n^2)$; See R.C. Hilborn, Chaos and Nonlinear Dynamics, Oxford University Press, New York, 1994, p. 234.

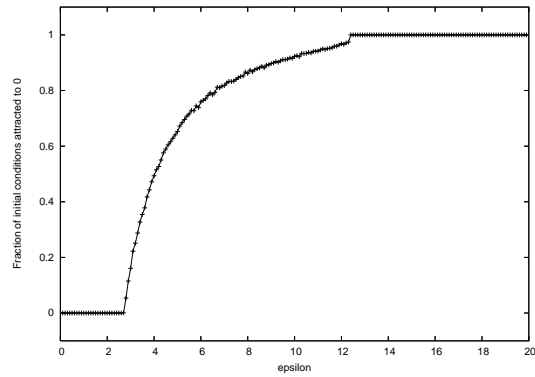


Figure 11: Fraction of initial conditions attracted to the fixed point $x^* = 0$, for varying values of ϵ for $a = 3.7$.

- [7] E. Ott, *Chaos in Dynamical Systems*, Cambridge University Press, Cambridge, 1993, p.63; K. Coffman, W.D. McCormick, H. Swinney, *Phys. Rev. Lett.* 56 (1986) 999.

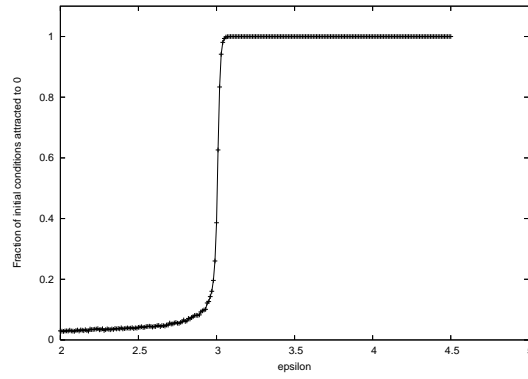


Figure 12: Fraction of initial conditions attracted to the fixed point $x^* = 0$, for varying values of ϵ for $a = 4$.

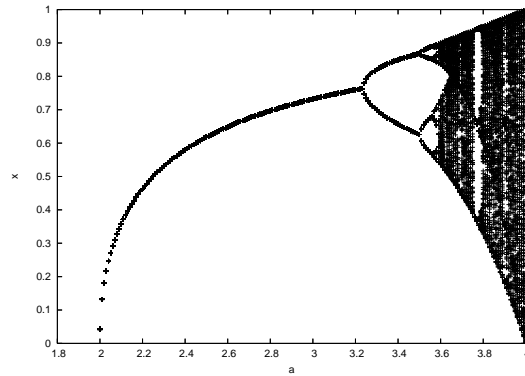


Figure 13: Bifurcation diagram of the map with respect to a for $\epsilon = 1$

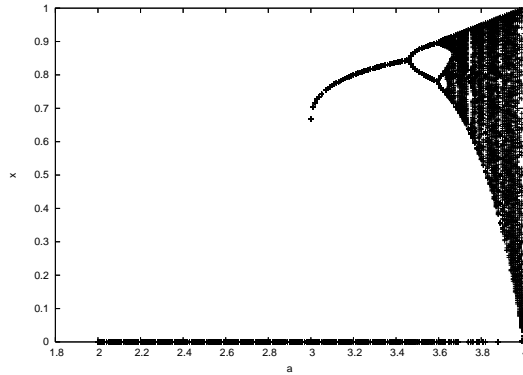


Figure 14: Bifurcation diagram of the map with respect to a for $\epsilon = 3$

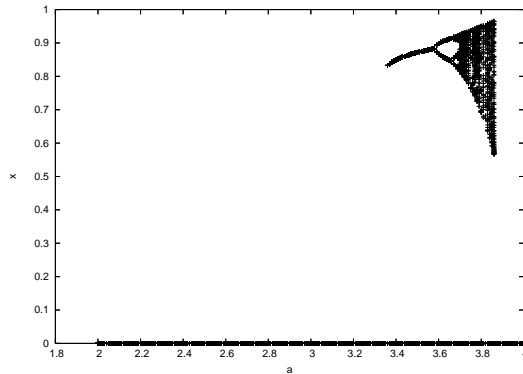


Figure 15: Bifurcation diagram of the map with respect to a for $\epsilon = 5$

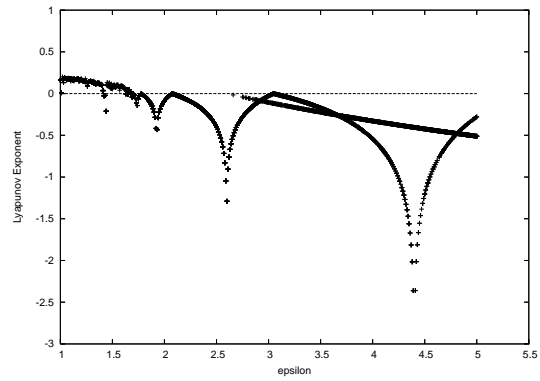


Figure 16: Lyapunov exponents with respect to ϵ for $a = 3.6$.

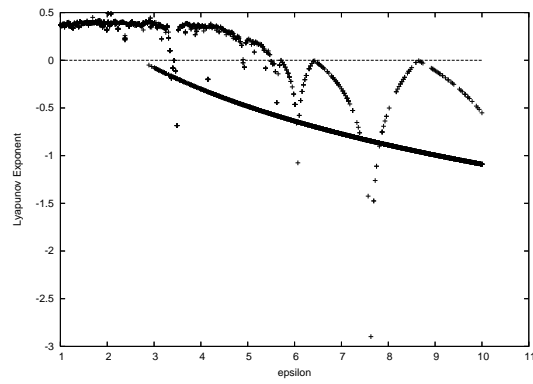


Figure 17: Lyapunov exponents with respect to ϵ for $a = 3.7$.

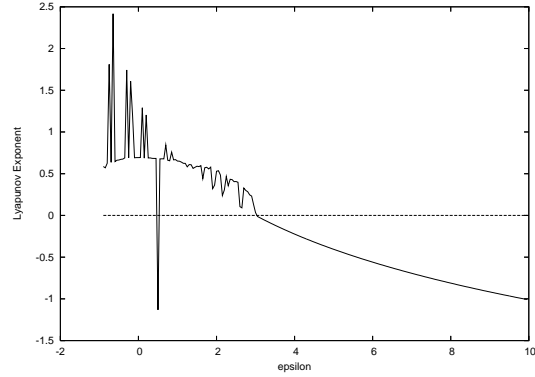


Figure 18: Lyapunov exponents with respect to ϵ for $a = 4$.

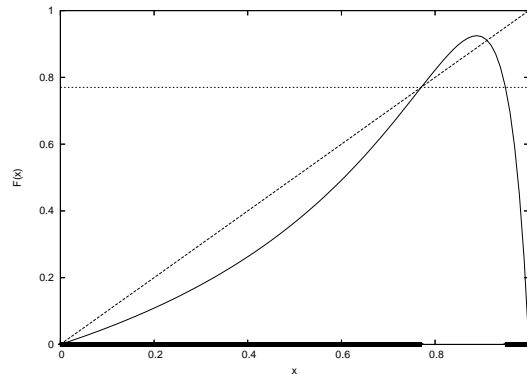


Figure 19: The form of the dynamical evolution function $F(x)$ with respect to x for $a = 3.7$ and $\epsilon = 7$. The dashed lines are: the $F(x) = x$ line (45° line) and the $F(x) = x^*$ line. The figure also shows the numerically obtained basin of attraction for the fixed point $x^* = 0$ as a black bar on the x -axis.